Decomposition of CO−H_2 over Graphite Nanofiber-Supported Iron and Iron−Copper Catalysts

O. C. Carneiro,† P. E. Anderson, N. M. Rodriguez, and R. T. K. Baker*

Catalytic Materials LLC, 1750 Washington Street, Holliston, Massachusetts 01746

Received: November 10, 2003; In Final Form: May 4, 2004

We investigated the effect on the catalytic behavior of iron and iron−copper induced by supporting the particles on "platelet" graphite nanofibers. The decomposition of CO/H_2 was selected as a probe reaction to ascertain the manner by which this unique type of support medium influences the activity and selectivity of the metal catalysts. For comparison purposes a corresponding set of experiments was carried out where the metal and bimetallic particles were dispersed on silica, a traditional support material. It was found that the overall performance of the graphite nanofiber-supported metal catalysts was superior to that of the corresponding silica-supported systems. Furthermore, it was significant to find that the structures of the solid carbon products were entirely different from those produced by the respective unsupported metal catalyst systems. These modifications in the behavior of the iron-containing particles are discussed in terms of the impact of a metal−support interaction.

Introduction

The performance of a supported catalyst system is governed to a large degree by a combination of the chemical nature of the reactant gas and the strength of the metal−support interaction.[1−8] These factors together with the reaction conditions can induce perturbations in the metal crystallites that modify both the reactivity and the selectivity of the catalyst and ultimately the pathway of the reaction.[9,10] Further modifications can result from the incorporation of a second metal to the formation of a bimetallic catalyst system. This procedure can alter the adsorptive and chemical properties of the catalyst, making its overall performance quite different from that of either of the respective monometallic entities.[11−14] It has been suggested that the observed enhancement in the performance exhibited by bimetallics can be attributed to the components being in a state that is more easily reduced due to a weakening of the strength of the metal−support interaction that ensues from alloy formation.[15]

The electrical conductivity properties of graphite offer some interesting possibilities when the material is used as a support medium for small metal particles.[16,17] Unfortunately, in its conventional form, graphite has limitations for this type of application due to the low surface area (1 m^2/g) and restricted number of reactive sites (edge regions). In this respect, significant improvements could be achieved if the material possessed a higher surface area coupled with a larger fraction of exposed edge sites and a smaller cross-sectional area. These conditions are met with certain types of graphite nanofibers (GNF), which are produced from the metal-catalyzed decomposition of selected carbon-containing gases at temperatures ranging from 500 to 900 °C.[18−20] Individual GNF are typically between 5 and 100 nm in width and 5 and 100 μm in length. These materials consist of graphene sheets aligned in definite directions that are dictated by the catalytic entity chosen for the growth process.[21] Unlike conventional graphite materials where for the most part only the basal plane is exposed, the structure of GNF can be such that only edge regions are revealed. The ability to tailor the structural characteristics of GNF so that the product has the blend of properties associated with active carbons (high surface area) and graphite (high electrical conductivity) makes these materials ideal for use as support media.[22]

Previous work from this group has demonstrated the dramatic improvements in catalytic performance of iron and iron−copper for the conversion of ethylene achieved by supporting the particles on "platelet" GNF compared to that found from similar metal loading on active carbon and γ-alumina.[23] An investigation by Salman and co-workers[24] showed that when nickel was supported on GNF, the gas-phase hydrogenation of crotonaldehyde to crotyl alcohol was significantly increased over that where the metal was dispersed on γ-alumina. This unexpected behavior was attributed to a combination of factors, the unusual crystallographic orientation of nickel particles, and the possibility that electronic perturbations were being induced in the metal from interactions with the electrically conductive nanofiber support media. In a recent study GNF-supported ruthenium−barium catalysts were found to exhibit remarkably high activity and stability for ammonia synthesis.[25] French workers[26] investigated the use of palladium dispersed on "herringbone" GNF for the liquid-phase hydrogenation of cinnamaldehyde and reported that with this catalyst system it was possible to achieve 98% selectivity to hydrocinnamaldehyde at 80 °C. This result was compared with that obtained with a commercial 5-wt % Pd/charcoal catalyst where the selectivity to hydrocinnamaldehyde was only 40% and the major product was phenylpropanol. They suggested that the enhancement in performance of the GNF-supported palladium catalyst could be due to the elimination of mass-transfer processes that are generally encountered with carbon-supported metals. They also invoked the existence of an unusual metal−support interaction; a finding that had previously been reported from XFAS studies of GNF-supported metals.[27]

The potential of GNF to function as an electrode for fuel-cell applications was tested using the electrochemical oxidation

* To whom correspondence should be addressed.
† Chemistry Department, Northeastern University, Boston, MA 02115.

10.1021/jp031235a CCC: $27.50
Published on Web 08/07/2004

of methanol at 40 °C as a probe reaction.[28] It was found that catalysts comprised of 5-wt % Pt supported on either "platelet" or "ribbon"-type GNFs exhibited activities comparable to those observed with 25-wt % platinum on Vulcan carbon. In addition, GNF-supported platinum particles were substantially more resistant to CO poisoning. The observed improvement in performance was attributed to the fact that the metal particles adopted specific crystallographic orientations when dispersed on the highly tailored GNF structures. Steigerwalt and co-workers[29] later carried out analogous studies in which they investigated the behavior of platinum−ruthenium (1:1) alloy clusters dispersed on "herringbone" GNF as the anode for a working direct methanol fuel cell. They reported that the performance of this electrode was 50% better than that of an unsupported platinum−ruthenium colloid of similar surface area and catalyst particle size.

The objective of the current investigation is to determine the impact of the chemical and physical properties of the support on the iron- and iron−copper-catalyzed decomposition of CO/H_2 mixtures. Specifically, we compared the catalytic activity and selectivity of the iron-containing particles dispersed on highly ordered "platelet" GNF with that observed for the same metal loading on amorphous silica. In these experiments both the gas-phase and solid-phase products have been examined.

Experimental Section

Materials. The "platelet" GNF employed as a catalyst support was prepared from the decomposition of a CO−H_2 gas mixture over an iron-based catalyst at 600 °C following a previously described protocol.[30] The metal catalyst used in the growth process of the nanofibers was removed by dissolution in a 1 M HCl solution over a period of 7 days. The nanofibers were then thoroughly washed in deionized water and dried in air at 110 °C. Subsequent X-ray diffraction analysis together with transmission electron microscopy failed to reveal the presence of any metal particles following this treatment. BET surface area measurements of the purified material gave values ranging from 60 to 80 m^2/g. Amorphous fumed silica (M-5 Cab-O-Sil) used as a support media had a BET surface area of 234 m^2/g.

The iron- and iron−copper-supported catalysts used in this investigation were prepared by a standard incipient wetness technique using an alcohol solution of iron and copper nitrates mixed in the desired ratios to give a 5 wt % total metal loading on the respective support media. The impregnates were dried overnight in air at 110 °C, calcined in air at 250 °C for 4 h to convert the metal nitrates to oxides, and then reduced at 350 °C in a 10% H_2/He mixture for 24 h. For the silica-supported metal catalysts this step was continued for a period of 72 h in order to ensure complete reduction of the oxides to the metallic state. After the reduction step, the samples were cooled to room temperature under flowing helium and then passivated in a 2% air−helium mixture for 1 h prior to removal from the reactor.

The gases used in this work, helium (99.999%), hydrogen (99.99%), and carbon monoxide (99.99%), were obtained from Air Products Inc. Traces of iron carbonyl were removed from the CO by passing the gas through a heated coil maintained at 200 °C. All gases were passed through molecular sieve traps to remove traces of water. Reagent-grade cupric nitrate [$Cu(NO_3)_2 \cdot 3H_2O$] and ferric nitrate [$Fe(NO_3)_3 \cdot 9H_2O$] were obtained from Fisher Scientific for the catalyst preparations.

Apparatus and Procedures. The apparatus used for the catalyst studies consisted of a horizontal quartz reactor tube, which was connected to gas supply lines and operated at atmospheric pressure. The gas flow to the reactor was precisely regulated by the use of MKS mass flow controllers, allowing a constant composition of a desired reactant feed to be delivered to the system. Catalyst samples (200 mg) were placed in a ceramic boat in the center of the reactor tube inside a Lindberg split furnace. Initially, the catalyst was reduced in a 10%H_2/He mixture while the temperature was raised to 350 °C (600 °C for silica-supported catalysts) and held at these respective levels for 2 h. The difference in the respective reduction steps results from the fact that one must avoid catalyzed hydrogenation of the nanofiber support, which will occur at temperatures in excess of 350 °C. On the other hand, it is necessary to carry out this step at higher temperatures to ensure complete reduction of the metals on the oxide support. Following the reduction step, the system was brought to the desired reaction temperature while the reactor was flushed with helium. At this stage a CO−H_2 (4:1) mixture was introduced into the system at a total flow rate of 100 cm^3/min, and then the reaction was allowed to proceed for various periods up to 5 h at temperatures ranging from 500 to 700 °C. The reaction was monitored as a function of time by sampling the inlet and outlet gas streams at regular intervals. The gas-phase products were analyzed by a Varian 3400 gas chromatography unit using a 30 m megabore (GS-Q) capillary column. The amounts of solid carbon generated by the catalyst were determined by weight difference and were within 5% of the value calculated from carbon mass balances.

The characteristics of the solid carbon products were determined from a combination of transmission electron microscopy (TEM). TEM examinations of the materials were performed in a JEOL 2000EXII instrument (point-to-point resolution of 0.18 nm). Transmission specimens were prepared by ultrasonic dispersion of a small quantity of a given sample in isobutanol and then application of a drop of the supernate onto a holey carbon film. Size distribution profiles were constructed from measurements of over 300 particles in each system. BET surface areas, calculated from nitrogen adsorption at −196 °C, were carried out on various materials using a Coulter Omnisorp 100CX automated unit.

Results

Flow Reactor Studies. The activity of the iron-based catalysts toward the formation of solid carbon was determined gravimetrically as a function of composition and reaction temperature for both support systems. Examination of the data for "platelet" GNF-supported catalysts presented in Figure 1 shows that the maximum yield of solid carbon occurs in the temperature range 550−600 °C. It is evident that the addition of copper to iron does not enhance the formation of carbon. Indeed, as the fraction of copper is progressively raised so the amount of solid carbon generated is decreased. Inspection of the corresponding data for the silica-supported iron-based particles shows the existence of some major differences to the former systems, Figure 2. In contrast to the "platelet" GNF-supported systems, in this case maximum activity for solid carbon growth is observed at about 500 °C and decreases at higher temperatures. Furthermore, the addition of 50% or less of copper to iron promotes the activity of the catalyst toward carbon formation. Despite this trend, however, it is clear that the amount of carbon produced from the GNF-supported iron catalysts is significantly higher than that obtained when silica is utilized as the carrier medium.

The gas-phase product distribution analysis was carried out for the decomposition of CO−H_2 (4:1) over the 5-wt % Fe supported on "platelet" GNF and silica, and these data are shown in Figures 3 and 4, respectively. Inspection of these plots reveals the existence of some fundamental differences between the two

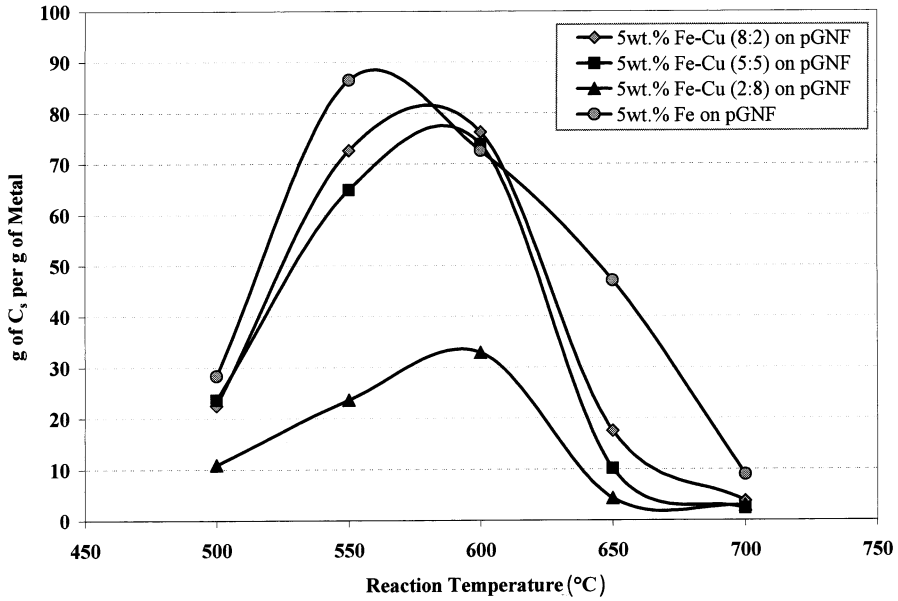

Figure 1. Amount of solid carbon formed as a function of reaction temperature from the interaction of "platelet" GNF-supported iron-containing particles with CO/H_2 (4:1).

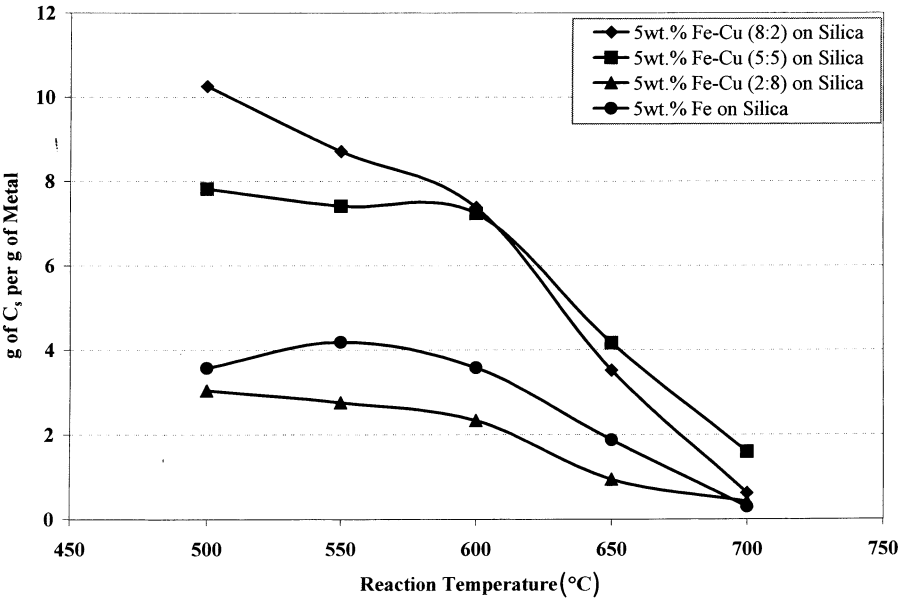

Figure 2. Amount of solid carbon formed as a function of reaction temperature from the interaction of silica-supported iron-containing particles with CO/H_2 (4:1).

catalyst systems. The decomposition of CO is about an order of magnitude higher over the Fe/GNF than the Fe/SiO_2 system. A further aspect concerns the amount of CO_2 that is generated in the two systems. When the reaction is conducted over Fe/GNF, the amount of CO_2 formed is close to that of solid carbon. In sharp contrast, when the decomposition reaction is carried out over Fe/SiO_2, the amounts of CO_2 are appreciably lower than those of solid carbon. These product relationships were found to persist for all the respective supported Fe−Cu bimetallic systems studied in this work as shown in Table 1. It is evident therefore that the nature of the support medium is exerting an impact on the selectivity of the reaction for all these systems.

Characterization Studies. Examination of the solid carbon products by TEM showed that for the most part the deposits consisted exclusively of carbon nanofibers. Examples of the typical size distributions of metal particles and the corresponding widths of the nanofibers formed after interaction of "platelet" GNF- and silica-supported Fe−Cu (8:2) with CO/H_2 (4:1) at 600 °C are presented in Figures 5 and 6, respectively. Inspection of these plots shows that when the iron-containing particles were dispersed on "platelet" GNF the size distribution was much broader than that obtained from the corresponding silica-supported system. Even larger deviations in distributions are observed when one examines the widths of nanofibers generated from these systems.

A summary of the average sizes of the iron-containing particles along with the average widths of the graphite nanofibers generated from the respective supported systems after reaction in CO/H_2 (4:1) at 600 °C for 1 h are presented in Tables 2 and 3, respectively. Inspection of these data reveals that dispersion of the metallic phase on "platelet" GNF always produced particles that were on average twice as large as those observed with the corresponding silica-supported systems. It is also evident that in all cases the widths of the nanofibers formed during the CO decomposition reaction was on average signifi-

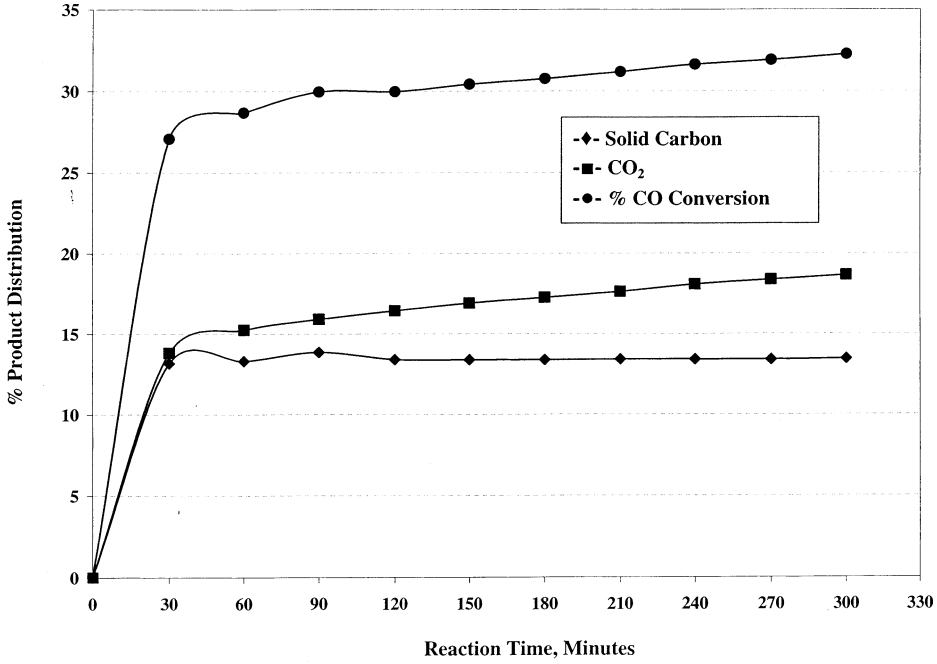

Figure 3. Product distribution as a function of reaction time for the decomposition of CO/H_2 (4:1) over 5 wt % Fe/GNF at 600 °C.

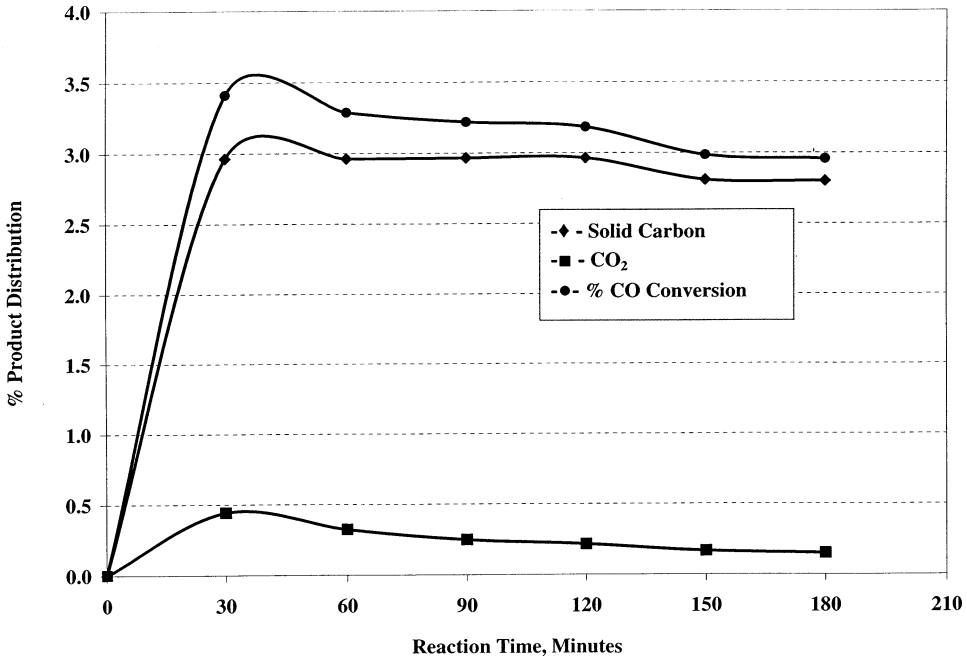

Figure 4. Product distribution as a function of reaction time for the decomposition of CO/H_2 (4:1) over 5 wt % Fe/silica at 600 °C.

TABLE 1: Product Distribution from Various wt % Fe−Cu Bimetallics Supported on "Platelet" GNF and Silica after Reaction in CO/H_2 (4:1) at 600 °C for 1 h

	SiO_2			"platelet" GNF		
	Fe−Cu (8:2)	Fe−Cu (5:5)	Fe−Cu (2:8)	Fe−Cu (8:2)	Fe−Cu (5:5)	Fe−Cu (2:8)
CO	97.2	96.6	93.3	74.1	74.8	78.9
CO_2	0.3	0.2	0.2	12.3	12.0	9.4
C_s	2.5	3.1	6.5	13.6	13.2	10.4

cantly wider than those of the initial metal catalyst particles. This relationship was most pronounced for the series of "platelet" GNF-supported iron and iron−copper catalysts. These findings would appear to indicate that the metal particles undergo a change in morphology prior to nanofiber growth. It should be stressed, however, that once the growth of the nanofibers commences, the width of the structures is approximately equal to that of the reconstructed catalyst particles. A further feature exhibited by the latter system is that as the fraction of copper in the bimetallic is progressively increased, there is a concomitant decrease in metal particle size and associated nanofiber width. It is significant that this aspect is not evident with the silica-supported iron-containing catalysts.

The morphology and overall structural characteristics of the nanofibers were ascertained from high-resolution TEM studies. The appearance of nanofibers grown from the interaction of 5-wt

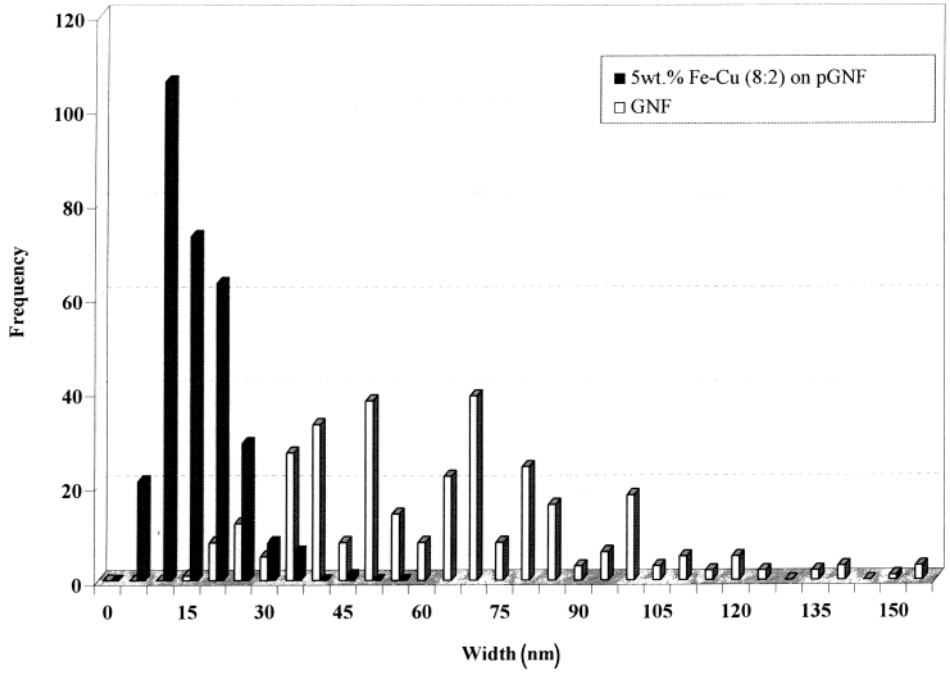

Figure 5. Size distributions of metal particles and the corresponding widths of the nanofibers formed after interaction of "platelet" GNF-supported Fe−Cu (8:2) with CO/H_2 (4:1) at 600 °C.

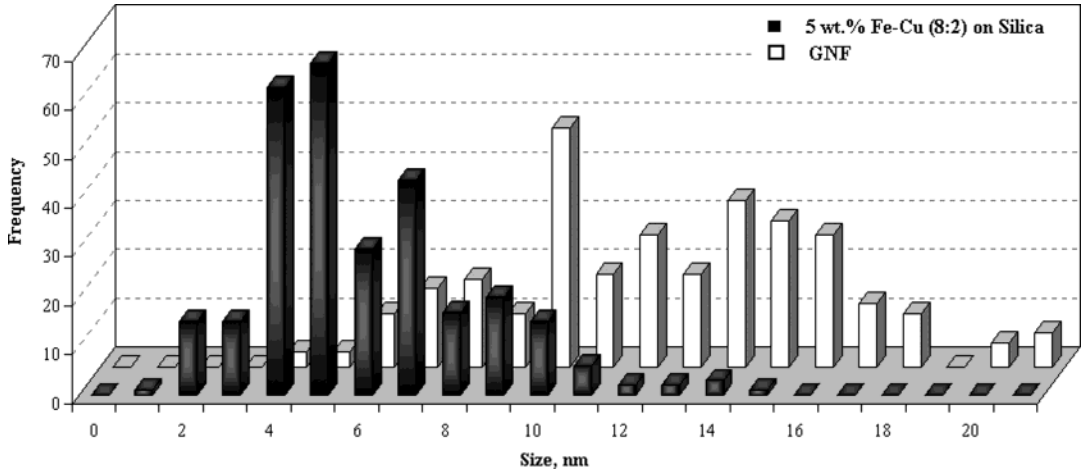

Figure 6. Size distributions of metal particles and the corresponding widths of the nanofibers formed after interaction of silica-supported Fe−Cu (8:2) with CO/H_2 (4:1) at 600 °C.

TABLE 2: Average Widths of Metal Particles Supported on "Platelet" GNF and GNF Structures Formed after Reaction in CO/H_2 (4:1) at 600 °C for 1 h

catalyst	average particle size (nm)	average GNF width (nm)
5 wt % Fe/pGNF	16.2	83.4
5 wt % Fe−Cu (8:2)/pGNF	13.1	62.9
5 wt % Fe−Cu (5:5)/pGNF	11.1	57.7
5 wt % Fe−Cu (2:8)/pGNF	12.7	43.2

TABLE 3: Average Widths of Metal Particles Supported on Silica and GNF Structures Formed after Reaction in CO/H_2 (4:1) at 600 °C for 1 h

catalyst	average particle size (nm)	average GNF width (nm)
5 wt % Fe/silica	5.2	11.8
5 wt % Fe−Cu (8:2)/silica	5.6	12.2
5 wt % Fe−Cu (5:5)/silica	7.6	17.9
5 wt % Fe−Cu (2:8)/silica	8.1	14.0

% Fe supported on "platelet" GNF is shown in the high-resolution electron micrograph, Figure 7. The structure can be described as a pseudo-"herringbone" edge arrangement surrounding a disordered core region. This type of nanofiber structure is to be contrasted with that of the "platelet" GNF support, which was generated from the interaction of Fe powder with CO/H_2 (4:1) at 600 °C and consists of graphite sheets aligned in direction perpendicular to the growth axis.[21] One can readily distinguish the secondary GNF growths from the parent "platelet" structures by the fact that the former always contained an associated catalyst particle at the growing end. When Fe/silica samples were treated in CO/H_2 (4:1) at 600 °C, electron microscopic examination revealed that the structures were quite different from those of the previous system. In this case, the nanofibers were very thin and exhibited a "beadlike" appearance as shown in Figure 8. Other workers have reported the formation of these types of nanofiber structures during the metal-catalyzed cracking of ethane and methane.[31,32] When GNF- and silica-supported 5 wt % Fe−Cu (8:2) were reacted in CO/H_2 (4:1) at 600 °C, the nanofibers were found to exhibit similar structural features to those formed from the corresponding supported iron systems when treated under the same conditions.

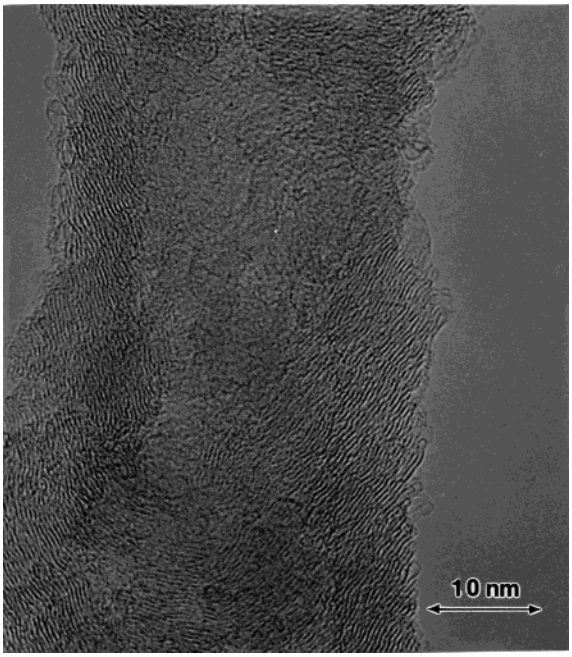

Figure 7. High-resolution electron micrograph showing the appearance of nanofibers grown from the interaction of 5-wt % Fe supported on "platelet" GNF.

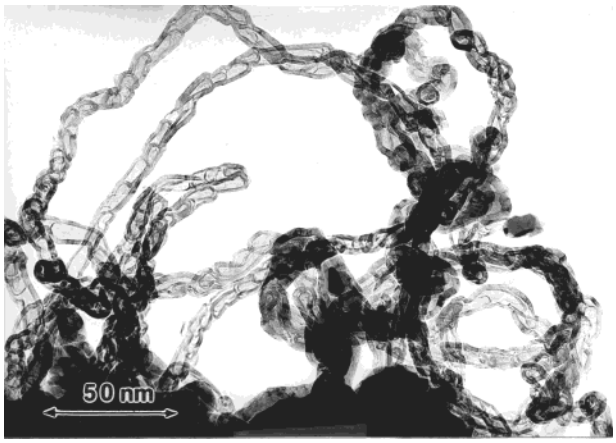

Figure 8. Transmission electron micrograph showing the "beadlike" nanofiber structures generated from the Fe/silica−CO/H_2 (4:1) system at 600 °C.

When the supported 5 wt % Fe−Cu (8:2) samples were heated at 700 °C and reacted in CO/H_2 (4:1), dramatic changes in the structural features of the nanofibers were observed. The high-resolution micrograph, Figure 9, shows the formation of "tubular"-type structures generated from the "platelet" GNF-supported bimetallic system. Close scrutiny of the edge regions reveals that the graphite sheets constituting these materials are aligned at a shallow angle with respect to the nanofiber growth axis. As a consequence, the arrangement allows for exposure of a small fraction of edges to the surrounding medium and potential to build chemical functionality on the surfaces. Under these conditions one also observes the formation of a "shell-like" deposit in which the metal catalyst particles appeared to be surrounded by several layers of graphite, Figure 10. Both types of structures were formed on the corresponding silica-supported Fe−Cu (8:2) samples; however, the relative widths and yields of the "tubular" structures were lower than on the GNF-supported particles. An analogous set of experiments was carried out with GNF- and silica-supported Fe−Cu (5:5) samples. Examination of these specimens showed that while

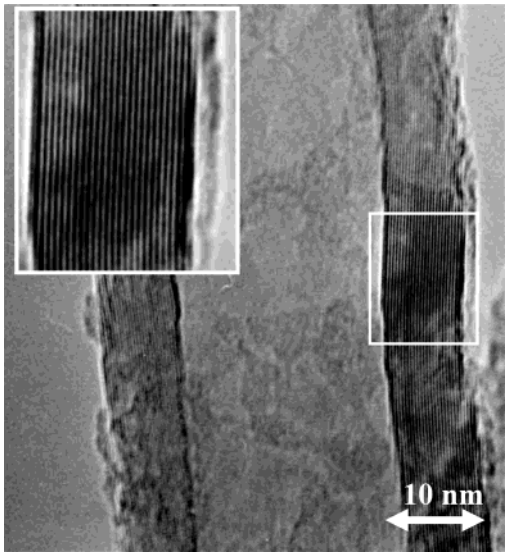

Figure 9. High-resolution micrograph showing the detailed structural features of "tubular" nanofibers produced from the interaction of "platelet" GNF-supported Fe−Cu (8:2) with CO/H_2 (4:1) at 700 °C.

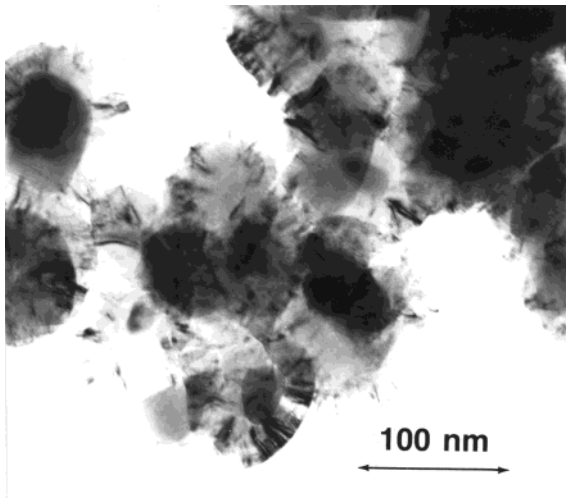

Figure 10. Transmission electron micrograph of the "shell-like" deposits formed on some of the GNF-supported Fe−Cu (8:2) particles during reaction with CO/H_2 (4:1) at 700 °C.

the characteristics of the nanofibers tended to follow the same trend as a function of temperature as those generated from the iron-rich catalysts, under these conditions the GNF tended to acquire a more disordered structure, an example is presented in Figure 11.

Discussion

It is interesting to observe that the silica-supported metal catalysts tend to deactivate after about 3 h on stream, whereas the corresponding "platelet" GNF-supported systems showed no loss of activity after 5 h of reaction. These observations are consistent with those reported by Rodriguez and co-workers,[23] who studied the conversion of hydrocarbons over Fe−Cu (7:3) and Fe particles supported on "platelet" GNF, active carbon, and γ-alumina. The performance of the GNF-supported iron-containing particles was far superior to that of either of the other two systems. Furthermore, it was found that the alumina-supported catalysts underwent severe deactivation after about 20 min on stream. In contrast, with the GNF-supported metal system, maximum activity was maintained for a prolonged period of time.

Figure 11. High-resolution micrograph showing the disordered appearance of nanofibers formed by silica-supported Fe−Cu (5:5) samples following interaction with CO/H_2 (4:1) at 600 °C.

This difference in catalyst behavior could not be rationalized on the basis of metal particle sizes. Alternative explanations were suggested that were predicated on the notion that the metal particles adopted a preferred crystallographic orientation when dispersed on the highly tailored nanofiber support.[23] Under these circumstances, particular metal faces would be exposed to the reactant environment. One might tentatively attribute this variation in catalyst behavior to differences in the morphological characteristics adopted by the metal particles on the two supports. A further factor that must be taken into consideration concerns the electronic properties of the respective support media. Since the "platelet" GNF is conductive in nature, the possibility exists for electron transfer between the metal particles and the support. Such a phenomenon is expected to exert an impact on the catalytic performance of the system. This condition would not be encountered with silica as it is an insulator.

Differences in the observed structural characteristics of the solid carbon products can also be attributed to the effect of the respective metal−support interactions. It is well established that the geometric shape and crystallographic arrangement of the exposed faces of the metal catalyst particles determines the alignment and perfection of graphite sheets constituting the nanofibers.[21] In this regard, reference should be made to the work of Yang and Chen,[33] who reported that in a nickel crystallite certain metal faces would preferentially decompose CO whereas another set of faces would favor the precipitation of dissolved carbon in the form of graphite. Clearly, the existence of electronic perturbations in the metal resulting from interactions with a conductive support is likely to exert an influence on the events occurring at both the metal−gas and metal−carbon interfaces. As a consequence, one would expect to find significant differences in the structural characteristics of the nanofibers generated from the two supported metal systems.

It is instructive to compare the structural characteristics of the nanofibers produced from the supported iron-based catalyst particles in the present study with those grown under the same reaction conditions from the corresponding unsupported powdered metal catalysts.[34] In the latter case, the Fe-rich Cu bimetallics all produced highly graphitic nanofibers that exhibited a "platelet" structure at 600 °C. When the reaction was carried out at 700 °C, the structural conformation changed from a "platelet" to "tubular" conformation that correlated with the α-Fe to γ-Fe phase change over this temperature range. Comparison of these data highlights the manner by which a support medium can exert an impact on catalytic behavior of small metal particles toward nanofiber growth. In this regard, it should be noted that Anderson and Rodriguez[35] reported a similar pattern of behavior during their study of nanofibers formed from the interaction of supported and unsupported nickel−iron particles with CO/H_2 mixtures.

Conclusions

The results of this investigation have demonstrated that the choice of the bimetallic catalyst, the nature of the support medium, and the temperature at which the reaction is performed are all factors that ultimately must be considered in the design of the structural architecture of graphite nanofibers. Furthermore, the dimensions of the nanofibers that are dictated by the sizes of the metal catalyst particles responsible for their growth are also dependent upon the nature of the interaction with the support.

References and Notes

(1) Schwarb, G. M. *Adv. Catal*. **1978**, *27*, 1.
(2) Solymosi, F. *Catal. Rev.-Sci. Eng*. **1967**, *1*, 233.
(3) Ichikawa, M. *J. Catal*. **1979**, *59*, 67.
(4) Verykios, X. E.; Stein, F. P.; Coughlin, R. W. *J. Catal*. **1980**, *66*, 147.
(5) Tauster, S. J.; Fung, S. C.; Baker, R. T. K.; Horsley, J. A. *Science* **1981**, *211*, 1121.
(6) Derouane, E. G.; Baker, R. T. K.; Dumesic, J. A.; Sherwood, R. D. *J. Catal*. **1981**, *69*, 101.
(7) Ruckenstein, E.; Chu, Y. F. *J. Catal*. **1979**, *59*, 109.
(8) Stevenson, S. A.; Dumesic, J. A.; Baker, R. T. K.; Ruckenstein, E. In *Metal-Support Interactions in Catalysis, Sintering and Redispersion*; Van Nostrand Reinhold: New York, 1987.
(9) Satterfield, C. N. In *Heterogeneous Catalysis in Practice*; McGraw-Hill: New York, 1980.
(10) Baker, R. T. K. *J. Adhes.* **1995**, *52*, 13.
(11) Sinfelt, J. H. In *Bimetallic Catalysts*; Exxon Monograph, John Wiley & Sons: New York, 1983.
(12) Sachtler, W. H. M.; van Santen, R. A. *Adv. Catal*. **1977**, *26*, 69.
(13) Sachtler, W. H. M. *Faraday Discuss. Chem. Soc*. **1981**, *72*, 7.
(14) Sinfelt, J. H.; Via, G.; Lytle, F. W. *Catal. Rev.-Sci. Eng*. **1984**, *26*, 81.
(15) Rao, C. N. R.; Kulkarni, G. U.; Kannan, K. R.; Chaturvedi, S. *J. Phys. Chem*. **1992**, *96*, 7379.
(16) Brownlie, I. C.; Fryer, J. R.; Webb, G. *J. Catal*. **1969**, *64*, 263.
(17) Gallezot, P.; Richard, D.; Bergeret, G. In *Novel Materials in Heterogeneous Catalysis*; Baker, R. T. K., Murrell, L. L., Eds.; ACS Symposium Series 437; American Chemical Society: Washington, D.C., 1990; p 150.
(18) Baker, R. T. K. In *Carbon Fibers, Filaments and Composites*; Figueiredo, J. L., et al., Eds.; NATO ASI Series 177; Kluwer: Dordrecht, 1990; p 405.
(19) Rodriguez, N. M. *J. Mater. Res*. **1993**, *8*, 3233.

(20) Laurent, C.; Flahaut, E.; Peigney, A.; Rousset, A. *New J. Chem*. **1998**, 1229.
(21) Rodriguez, N. M.; Chambers, A.; Baker, R. T. K. *Langmuir* **1995**, *11*, 3862.
(22) de Jong, K. P.; Geus, J. W. *Catal. Rev.-Sci. Eng*. **2000**, *42*, 481.
(23) Rodriguez, N. M.; Kim, M. S.; Baker, R. T. K. *J. Phys. Chem*. **1994**, *98*, 13108.
(24) Salman, F.; Park, C.; Baker, R. T. K. *Catal. Today* **1999**, *53*, 3862.
(25) Liang, C.; Li, Z.; Qiu, J.; Li, C. *J. Catal*. **2002**, *211*, 278.
(26) Pham-Huu, C.; Keller, N.; Ehret, G.; Charbonniere, L. J.; Ziessel, R.; Ledoux, M. J. *J. Mol. Catal., A: Chem.* **2001**, *170*, 155.
(27) Mojet, B. L.; Hoogenraad, M. S.; van Dillen, A. J.; Geus, J. W.; Koningsberger, D. C. *J. Chem. Soc., Faraday Trans*. **1997**, *93*, 4371.
(28) Bessel, C. A.; Laubernds, K.; Rodriguez, N. M.; Baker, R. T. K. *J. Phys. Chem. B* **2001**, *105*, 1115.
(29) Steigerwalt, E. S.; Deluga, G. A.; Lukehart, C. M. *J. Phys. Chem. B* **2001**, *105*, 8097.
(30) Rodriguez, N. M.; Kim, M. S.; Baker, R. T. K. *J. Catal*. **1993**, *144*, 93.
(31) Rodriguez, N. M.; Kim, M. S.; Fortin, F.; Mochida, I.; Baker, R. T. K. *Appl. Catal., A: Gen.* **1997**, *148*, 265.
(32) Zhang, T.; Amiridis, M. D. *Appl. Catal., A: Gen.* **1998**, *167*, 161.
(33) Yang, R. T.; Chen, J. P. *J. Catal*. **1989**, *115*, 52.
(34) Carneiro, O. C.; Kim, M. S.; Yim, J. B.; Rodriguez, N. M.; Baker, R. T. K. *J. Phys. Chem. B* **2003**, *107*, 4237.
(35) Anderson, P. E.; Rodriguez, N. M. *J. Mater. Res*. **1999**, *14*, 2912.